https://doi.org/10.17113/ftb.64.03.26.9373 original scientific paper

Structural, Functional and Antioxidant Properties of Soy Protein Concentrates Enriched with Black Mulberry Pomace

Running head: Soy Protein Concentrate Enriched with Mulberry Pomace

Nevena Barać[1], Biljana Rabrenović[1], Ivana Sredović Ignjatović[1], Steva Lević[1], Vladimir Pavlović[1], Slađana Žilić[2], Danka Milovanović[2] and Miroljub Barać[1*]

[1]Faculty of Agriculture, University of Belgrade, Nemanjina 6, 11080 Belgrade, Serbia
[2]Maize Research Institute, Slobodana Bajića 1, Zemun polje, 11185 Belgrade, Serbia

Received: 16 September 2025
Accepted: 10 April 2026

SUMMARY

Research background. The incorporation of fruit processing residues into protein-rich ingredients is gaining attention as a sustainable strategy to enhance the nutritional and functional value of plant-based formulations. However, the influence of black mulberry pomace addition on protein matrix structure, functionality, and digestibility remains insufficiently explored. This study investigates the potential of using black mulberry pomace as a co-ingredient to modify and improve the characteristics of soy protein concentrate derived from moderately toasted soy flour.

Experimental approach. Soy protein concentrates were obtained by washing soy flour with ethanol after blending it with increasing proportions of black mulberry pomace. The prepared samples were examined for their chemical composition, *in vitro* digestibility, hydration and emulsifying properties, and antioxidant potential using standard radical scavenging and metal-chelating assays. Structural characteristics were investigated using infrared spectroscopy and electron microscopy.

*Corresponding author:
Phone:+387114413268
E-mail: baracm@agrif.bg.ac.rs

Relationships among compositional, functional, and antioxidant parameters were explored using multivariate statistical analysis.

Results and conclusions. Black mulberry pomace addition improved hydration and emulsifying properties at lower inclusion levels, while enhancing antioxidant potential through phenolic incorporation. These enhancements were attributed to interactions between phenolic compounds and protein structures, confirmed by spectroscopic and microscopic evidence. However, higher pomace concentrations negatively affected protein digestibility, likely due to matrix densification and aggregation. Correlation and multivariate analyses confirmed close associations between antioxidant activity, protein solubility, and techno-functional performance. These findings suggest that low to moderate pomace levels are sufficient to induce positive changes without compromising digestibility.

Novelty and scientific contribution. This work provides new insights into the dual role of black mulberry pomace as a functional and antioxidant-enhancing agent in plant protein systems. It highlights a sustainable approach for the development of value-added protein ingredients by integrating underutilised agri-food residues. The comprehensive combination of chemical, functional, and structural analysis presented in this study contributes to a better understanding of how co-ingredient interactions can shape the bio-functional performance of soy-based matrices.

Keywords: soy protein concentrate; black mulberry pomace; polyphenol-protein interactions; antioxidant properties; techno-functional performance; sustainable co-ingredients

INTRODUCTION

The growing demand for sustainable and health-promoting food ingredients has intensified interest in plant-based proteins as alternatives to animal-derived products. Soy protein is particularly valued for its favourable amino acid composition, high digestibility, and versatile functionality in food systems. Among soy-derived ingredients, soy protein concentrates (SPCs) are widely utilised due to their high protein content and favourable techno-functional properties including water- and oil-holding capacity, emulsifying capacity, and emulsion stability [*1*].

Simultaneously, the agri-food industry generates large amounts of plant-based by-products that are rich in fibre, organic acids, vitamins, minerals and bioactive compounds but often remain underutilised. Recent studies [*2-5*] report that pomaces from apple, grape, citrus and berries can enhance nutritional value and modulate technological and sensory properties when incorporated into cereal, bakery, dairy, or extruded products. In addition to their fibre fraction, pomaces provide

polyphenols, including flavonoids and anthocyanins, which exhibit antioxidant, anti-inflammatory, and other bioactivities that can be harnessed to design clean-label and health-oriented foods [*6,7*].

Black mulberry (*Morus nigra* L.) pomace, a major residue from juice and wine production, contains abundant polyphenols, flavonoids, and dietary fibre, and exhibits promising antioxidant potential [*8*]. Its valorisation is in line with circular economy principles and offers opportunities for the development of novel functional ingredients. However, its potential has not yet been fully explored.

A promising strategy for the next generation of SPCs can be the integration of fruit-derived materials during SPC manufacture so as to co-extract and/or retain bioactive compounds while tailoring functionality. The conventional alcohol-washing step efficiently removes soluble carbohydrates from soy, but it may also remove endogenous phytochemicals [*1*]. Introducing a polyphenol-rich fruit fraction during extraction could offset such losses by supplying additional phenolics and fibre and by enabling *in-situ* formation of polyphenol-protein associations. Depending on the phenolic class and processing conditions, these non-covalent and covalent interactions can alter protein conformation, surface hydrophobicity and charge with resulting effects on solubility, gelation, emulsifying activity, and even protein digestibility [*9,10*].

In this context, co-processing soy flour with black mulberry pomace during SPC manufacture is expected to yield products with enhanced phenolic content, antioxidant capacity, and potentially improved functional properties, while contributing to sustainable by-product utilisation. The methodology used in this study is particularly relevant because aqueous-ethanol extraction is already a well-established industrial process for SPC production. Integrating fruit pomace at this stage requires no major process redesign yet allows direct incorporation of valuable bioactive compounds into the protein matrix. This approach also provides a unique model system for studying the effects of polyphenol-protein interactions formed under realistic industrial processing conditions.

Therefore, the aim of this study was to investigate the chemical composition, techno-functional, antioxidant, and microstructural properties of SPCs obtained by ethanol extraction of soy flour co-processed with graded levels (0–10 %, by mass) of black mulberry pomace. Protein and sugar contents, total phenolic content (TPC), total flavonoid content (TFC), colour parameters, antioxidant capacity (DPPH, ABTS), *in vitro* protein digestibility, and functional properties (water- and oil-holding capacity, emulsifying capacity and emulsion stability) were determined. Fourier transform infrared (FTIR) spectroscopy and scanning electron microscopy (SEM) were employed to elucidate structural and surface modifications. This integrated approach is expected to provide new insights into the functionalisation of SPCs through co-processing with polyphenol- and fibre-rich fruit by-products, thereby supporting the development of multifunctional, clean-label plant protein ingredients.

MATERIALS AND METHODS

Materials

Moderately toasted defatted soy flour (Bp10L, Bankom doo, Belgrade, Serbia) was used for the preparation of soy protein concentrates (SPCs). Fresh black mulberry (*Morus nigra* L.) pomace, a by-product obtained after cold-pressed juice production, was collected and stored at −18 °C until further use. Its average chemical composition on a dry matter basis was as follows: total sugars 17.8 %, crude fibre 57.0 %, crude fat 9.5 %, protein 8.7 % (by mass), total phenolic content 6.06 mg gallic acid equivalents (GAE)/g, total flavonoid content 2.61 mg quercetin equivalents (QE)/g, and anthocyanin content 150 µg cyanidin-3-glucoside (Cy-3-G)/100 g (unpublished data).

Preparation of soy protein concentrates

Defatted soy flour was blended with mulberry pomace at mass fractions of 0, 1, 2, 5 and 10 %. The mixtures were extracted with 65 % (by volume) aqueous ethanol for 60 min at 40 °C using a magnetic stirrer to ensure continuous agitation. Following extraction, the suspensions were centrifuged at 2500×*g* for 10 min (DM0412, DLAB, Beijing, China). The resulting pellets were rinsed with 50 mL of the same ethanol solution and centrifuged again under identical conditions. The supernatants were discarded, and the pellets, representing the soy protein concentrates, were dried in a laboratory oven at 50 °C for 6 h. The dried material was then ground into a fine powder using a laboratory mill (A11 Basic, IKA, Staufen, Germany). All samples were prepared in triplicate using the same batch of soy flour and mulberry pomace.

Chemical composition analysis

The chemical composition of SPCs was determined using standard analytical procedures. Total nitrogen (TN) was analysed using the Kjeldahl method and expressed as total protein per dry matter (TP/DM) [*11*]. The method is based on acid digestion of the sample, followed by distillation and titration of released ammonia to quantify nitrogen content. Dry matter was determined by oven-drying at 105 °C to constant mass [*12*], while the fat content was measured by Soxhlet extraction using n-hexane [*13*]. Crude fibre content was determined according to the standard AOAC procedure [*14*], based on sequential acid and alkaline digestion of the sample residue.

Water-soluble and acid-hydrolysable sugars were quantified using the phenol-sulphuric acid method [*15*]. Briefly, 1 g of SPC sample was extracted with 10 mL of deionised water (Milli-Q) for 1 h

and centrifuged at 2500×*g* (DM0412, DLAB, Beijing, China) for 10 min. The supernatant was used to determine water-soluble sugars. The pellet was rinsed with 5 mL of deionised water, centrifuged under the same conditions, and hydrolysed with 10 mL of 0.5 mol/L H_2SO_4 in a boiling water bath for 2 h. After cooling, the mixture was centrifuged again, and the supernatant was used for the determination of acid-hydrolysable sugars. Absorbance was measured at 490 nm using a UV-Vis spectrophotometer (UV-1800, Shimadzu, Kyoto, Japan). Sugar content was calculated from a glucose calibration curve and expressed as g/100 g dry matter.

Water-soluble protein content was determined using the Bradford method [*16*], with bovine serum albumin (BSA, Sigma-Aldrich, St Louis, USA) as a standard. Results were expressed as g/100 g dry matter.

Determination of total phenolic and flavonoid content

Total phenolic content (TPC) of the SPCs was determined using the Folin–Ciocalteu method, as described by Kostić *et al*. [*17*], with slight modifications. Briefly, 0.1 g of powdered SPC was extracted in 10 mL of deionised water using a vortex mixer for 1 h at room temperature. The extracts were centrifuged at 2400×*g* for 10 min (DM0412, DLAB, Beijing, China). A volume of 182 µL of the undiluted extract was mixed with 909 µL of Folin (Sigma-Aldrich, St Louis, USA) working solution (1:9 dilution). After 5 min, 909 µL of 7.5% sodium carbonate solution was added. The mixtures were kept in the dark for 90 min, after which absorbance was measured at 765 nm using a UV-Vis spectrophotometer (UV-1800, Shimadzu, Kyoto, Japan). TPC was expressed as milligrams of gallic acid (Sigma-Aldrich, St Louis, USA) equivalents per gram of dry matter (mg GAE/g dm), based on a gallic acid calibration curve prepared in the same manner.

Total flavonoid content (TFC) was determined according to the method of Žilić *et al*. [*18*], with slight modifications. A quantity of 100 mg of SPC sample was extracted with 10 mL of 70 % (by volume) aqueous acetone for 30 min using a mechanical shaker, followed by centrifugation at 2500×*g* for 10 min (DMO412, DLAB, China). The absorbance of the supernatant was measured at 360 nm using a UV-Vis spectrophotometer (UV-1800, Shimadzu, Kyoto, Japan). TFC was expressed as milligrams of quercetin (Sigma-Aldrich, St Louis, USA) equivalents per gram of dry matter (mg QE/g) based on a quercetin calibration curve.

.

Determination of total anthocyanin content

Total anthocyanin content (TAC) was determined according to the pH differential method as suggested by Giusti and Wrolstad [*19*]. Briefly, 2 g of SPC sample was extracted with 20 mL of 95 % ethanol containing 1 % (by volume) HCl. The mixture was stirred on a mechanical shaker for 1 h at room temperature and then centrifuged at 2500×*g* (DMO412, DLAB, China) for 10 min. The absorbance of the clear supernatant was measured at 520 nm and 700 nm (UV-1800, Shimadzu, Kyoto, Japan) in two buffer systems (potassium chloride buffer, pH=1.0, and sodium acetate buffer, pH=4.5) using a quartz cuvette with a 1 cm path length.

TAC was calculated using the following equation:

$$TAC=(A_{520\ nm}-A_{700\ nm})_{pH=1.0}-(A_{520\ nm}-A_{700\ nm})_{pH=4.5} \quad /1/$$

The results were expressed as mg of cyanidin-3-glucoside equivalents per 100 g of dry sample using a molar absorptivity (ε=26.900 L/(mol·cm)) and molecular mass of 449.2 g/mol.

Determination of antioxidant properties

The antioxidant properties of SPCs enriched with mulberry pomace were assessed by evaluating Fe(II) chelation, ABTS and DPPH radical scavenging activities. Fe(II) chelating ability was determined according to the method of Meira *et al*. [*20*]. Briefly, 100 mg of powdered SPC was extracted with 10 mL of deionised water using a vortex mixer for 30 min, followed by centrifugation at 2500×*g* for 15 min (DM0412, DLAB, Beijing, China). A volume of 1 mL of the clear extract was mixed with 3.7 mL of deionised water, 0.1 mL of 2 mmol/L FeSO4, and 0.2 mL of 5 mmol/L ferrozine (Sigma-Aldrich, St Louis, USA). After 10 min, the absorbance was measured at 562 nm. A control sample was prepared by replacing the extract with deionised water. The chelating ability (%) was calculated as:

$$\text{Chelating ability}=(1-A_{sample}/A_{control})\cdot 100 \quad /2/$$

ABTS radical scavenging activity was assessed using the method of Arnao *et al*. [*21*]. A stock solution of ABTS (Sigma-Aldrich, St Louis, USA) was prepared by mixing 7 mmol/L ABTS with 2.45 mmol/L potassium persulfate and allowing it to stand in the dark for 16 h. The working solution was obtained by diluting the stock solution with methanol to an absorbance of 0.70–0.80 at 734 nm. Then, 1 mL of the ABTS working solution was mixed with 50 µL of SPC extract, vortexed, and incubated in the dark for 7 min. A control was prepared using 50 µL of deionised water instead of the extract. Absorbance was measured at 734 nm. The ABTS scavenging activity (%) was calculated as follows:

$$\text{ABTS scavenging activity}=[(A_{control}-A_{sample})/A_{control}]\cdot 100 \quad /3/$$

A calibration curve was prepared using Trolox (Sigma-Aldrich, St Louis, USA) standards (10-100 μg/mL), and results were expressed as μmolTrolox equivalents/g DM.

DPPH radical scavenging activity was evaluated according to Kostić *et al*. [*17*]. A volume of 105 μL of the water extract was mixed with 840 μL of freshly prepared DPPH (Merck, Darmstadt, Germany) working solution. The mixture was incubated in the dark for 30 min, and the absorbance was measured at 515 nm (UV-1800, Shimadzu, Kyoto, Japan). The DPPH scavenging capacity was expressed as μmol Trolox equivalents per gram of dry sample.

Color measurement

Color parameters (CIE Lab*) were measured using a Chroma Meter CR-400 (Konica Minolta, Tokyo, Japan), calibrated with a white standard (CM-A70). Ground samples were placed in an optical glass cell, and measurements were performed using SpectraMagic NX software [*22*]. Chroma (*C**), hue angle (*h*°) and total color difference (Δ*E*) were calculated as:

$$C^*=\sqrt{(a^2 + b^2)} \quad /4/$$

$$h^\circ=\arctan2\,(b^*,a^*) \quad /5/$$

$$\Delta E=\sqrt{[(L^*-L_0^*)^2 + (a^*-a_0^*)^2 + (b^*-b_0^*)^2]} \quad /6/$$

where *L** is lightness, *a** is red/green coordinate (positive values indicate redness, negative greenness), *b** is yellow/blue coordinate (positive values indicate yellowness, negative blueness), *C** is chroma (colour saturation), *h*° is hue angle (tone of the colour), Δ*E* is total colour difference between treated sample and control (0 % black mulberry pomace), and L_0^*, a_0^* and b_0^* are colour parameters of the control sample. Results were reported as mean values from three independent measurements.

Determination of techno-functional properties

Emulsifying properties of SPC were assayed using the turbidimetric method as described by Barać *et al*. [*23*]. Briefly, pure sunflower oil (15 mL) and 45 mL 1 % water suspension of SPC were homogenized in a mechanical homogenizer for 1 min at the highest settings (7500×*g*). A volume of 50 μL of emulsions was pipetted from the bottom of the container at 0 and 10 min after homogenization and diluted with 10 mL of 0.1 % SDS (Sigma-Aldrich, St Louis, USA) solution. Absorbances of these diluted emulsions were measured at 500 nm. Emulsifying activity index (EAI) and emulsifying stability

index (ESI) were calculated using values for the absorbance at 0 (A_0) and 10 min (A_{10}) after emulsion formation. Emulsifying properties were expressed as EAI (m^2/g) and ESI (min) according to the following equations:

$$EAI=2T(A_0 \cdot DF/\gamma \cdot \varphi \cdot 200) \quad /7/$$

where T is 2.303, A_0 is the absorbance measured immediately after emulsion formation, DF is the dilution factor 200, γ is the protein mass concentration of protein/unit volume (g/mL) of aqueous phase before emulsion formation, and φ is oil volume fraction (calculated by drying the emulsion).

$$ESI=A_0 \cdot \Delta t/\Delta A \quad /8/$$

where Δt is 10 min and ΔA is A_0-A_{10}.

Water-holding capacity (WHC) and oil-holding capacity (OHC) were assayed as suggested by Gouw *et al*. [*24*]. In a Falcon tube, 0.5 g of SPC was mixed with 10 mL of pure sunflower oil, left overnight at room temperature, centrifuged (DMO412, DLAB, China) at 1500·*g* for 5 min, and the excess of oil was carefully decanted. The sample with the adsorbed oil was reweighed, and OHC was expressed as g oil per g dry matter.

In a Falcon tube, 1 g of SPC was mixed with 50 mL of deionized water for 5 min, centrifuged at 4000·*g* (DMO412, DLAB, Beijing, China) for 10 min, the excess of water was carefully decanted, and the sample was reweighed. The WHC was expressed as g water per g dry matter.

In vitro multistep enzymatic digestion

Digestibility of SPCs was assessed using a multistep *in vitro* digestion protocol simulating oral, gastric, duodenal, and colonic phases based on Papillo *et al*. [*25*] with modifications from Hamzalıoğlu and Gökmen [*26*]. Simulated salivary (SSF), gastric (SGF), and duodenal fluids (SDF) were prepared accordingly. A mass of 5 g of sample was sequentially treated with SSF, SGF with pepsin (pH=2.0, 2 h, 37 °C; Sigma-Aldrich, St Louis, USA), SDF with pancreatin and bile salts (pH=7.5, 2 h, 37 °C), followed by protease (1 h) and Viscozyme L (16 h; Novozymes, Bagsværd, Denmark) incubations at 37 °C with shaking. The digested residue was filtered, air-dried (2 h), and oven-dried at 105 °C (4 h) to constant mass. Digestibility was expressed as the percentage reduction of dry mass.

Fourier transform infrared spectroscopy (FTIR)

FTIR spectra of SFCs were recorded at room temperature using a FTIR spectrophotometer IRAffinity-1 (Shimadzu, Kyoto, Japan). Before analysis, the samples were mixed with potassium bromide and compressed into pellets using a hydraulic press. All spectra were recorded in the spectral range 4000–600 cm^{-1}, at a resolution of 4 cm^{-1}. Each sample was scanned 100 times while a background was recorded before analyzing each sample using a pure KBr pellet. Peak positions (ν_{max}) for O-H, C-H, amide I, amide II, amide III, and C-O stretching bands were identified via peak-picking. Shift ($\Delta\nu$) was calculated relative to control (0 % pomace). The intensity ratio I_{1650}/I_{1540} was computed as the ratio of absorbances at amide I and amide II, as a proxy for secondary structural assessment, following standard FTIR methodologies [*27*].

Scanning electron microscopy (SEM)

The surface morphology of the samples was examined using a scanning electron microscope (JSM-6390LV, JEOL Ltd., Tokyo, Japan). Prior to analysis, the samples were mounted on aluminum stubs using double-sided carbon tape and sputter-coated with a thin layer of gold to improve conductivity. Micrographs were captured at various magnifications (100×, 300×, 500×, and 1200×) under a high vacuum mode and an accelerating voltage of 15 kV.

Statistical analysis

All experiments were conducted in triplicate, and results are expressed as mean±standard deviation (S.D.). One-way analysis of variance (ANOVA) followed by Tukey's HSD *post hoc* test was performed to assess significant differences ($p<0.05$) among sample groups using IBM SPSS Statistics v. 26.0 [*28*]. Multivariate analyses, including principal component analysis (PCA), Pearson's correlation analysis, and hierarchical cluster analysis (HCA), were carried out using Python programming language v. [*29*] with relevant packages: pandas for data handling, scikit-learn for PCA and clustering, and seaborn for data visualization.

RESULTS AND DISCUSSION

Chemical composition of soy protein concentrates

The chemical composition of SPCs obtained by ethanol extraction from defatted soybean flour blended with different proportions of black mulberry pomace is presented in Table 1. The enrichment with pomace affected protein, carbohydrate, fibre, and oil fractions significantly ($p<0.05$).

Table 1

The control sample (0 % pomace) contained 71.92 g/100 g of protein, which is consistent with previously reported values (≥70 %) for ethanol-washed SPCs [*30*]. The highest protein level was detected at 2 % pomace, significantly ($p<0.05$) exceeding all other samples. At higher pomace levels (5 and 10 %), total protein mass fraction declined, approaching values similar to those of the control. This biphasic trend suggests that moderate pomace addition may favour protein retention, whereas larger proportions exert a dilution effect associated with increased fibre incorporation. The soluble protein fraction followed a different trend: all enriched samples showed significantly ($p<0.05$) higher values (8.66–9.89 g/100 g) than the control (5.71 g/100 g). This enhancement is most likely due to the release of low-molecular-mass proteins and their potential interactions with polyphenols, which may unfold protein structures and improve solubility [*9*].

Carbohydrates also reflected the influence of pomace. Water-soluble sugars doubled from 0.33 g/100 g in the control to 0.67 g/100 g at 10 % pomace, while acid-hydrolysable sugars tripled (6.40 to 18.86 g/100 g). These data indicate that the pomace introduced both easily extractable and more resistant polysaccharide fractions. Fibre increased markedly and proportionally to pomace level, from 4.82 to 11.34 g/100 g, consistent with the fibrous composition of mulberry by-products. Beyond nutritional benefits, this enrichment is expected to modulate techno-functional behaviour such as hydration and oil-binding, and to contribute to physiological effects related to digestive regulation and glycaemic control [*31,32*].

Oil content increased more moderately, from 0.75 g/100 g (control) to 1.30 g/100 g (10 % pomace). The additional lipids originated from the seed fraction of mulberry pomace, reported to contain 27.5–33 % crude oil rich in linoleic acid (~73.7 %), with smaller proportions of palmitic, oleic, and stearic acids, along with α-tocopherol and phytosterols [*33*]. These compounds are known for their antioxidant and cholesterol-lowering properties [*34*].

These results showed that mulberry pomace altered SPC composition in a manner that combines higher soluble protein with increased fibre, sugars, and minor lipophilic bioactive compounds. An inclusion of around 2 % appears optimal for maximising protein yield, whereas higher levels progressively enrich the carbohydrate and fibre fractions, setting the basis for changes observed in techno-functional, antioxidant, and digestibility properties.

Techno-functional properties

The effects of black mulberry pomace incorporation on the techno-functional properties of SPCs are presented in Fig. 1. Considering the compositional differences described above, these

properties were evaluated in terms of water-holding capacity (WHC), oil-holding capacity (OHC), emulsifying activity index (EAI) and emulsion stability index (ESI).

Fig. 1

The WHC exhibited a non-linear trend with the highest value at 1 % inclusion (Fig. 1c), followed by a decrease at 2 %. At higher pomace levels (5 and 10 %), WHC values increased again, reaching (3.8±0.02) g/g at 10 %. This pattern indicates that a small to moderate fibre fraction most effectively enhances hydration capacity, likely through the formation of a denser protein-fibre network and the presence of more hydrophilic binding sites. At 10 %, WHC remained higher than the control, reflecting the strong contribution of total fibre content and its swelling ability. Comparable trends have been reported for mulberry pomace-fortified yoghurt, where WHC was improved relative to the control. Du *et al*. [*5*] showed that the addition of mulberry pomace at 1–3 % increased water-holding capacity by approximately 10–20 %. A comparable pattern was noted for OHC, which was highest at 1 % and 10 % inclusion ((1.4±0.02) g/g), while intermediate values (2 and 5 %) remained constant at 1.3 g/g (Fig. 1d). This suggests that both moderate and higher inclusions provide sufficient hydrophobic sites (fibre porosity and exposure of hydrophobic protein regions via polyphenol interactions) for oil retention, while intermediate levels appear saturated. Such functional enhancements are consistent with the opinion of Elleuch *et al*. [*35*]. These authors highlight that plant-derived fibres can promote oil binding through combined structural (porosity, surface area) and surface property (hydrophobic interactions) effects, a mechanism that can also operate in composite systems containing proteins.

The EAI significantly increased with pomace incorporation ($p<0.05$), reaching a maximum at 1 % inclusion ((116.35±4.0) m^2/g; Fig. 1a). Samples with 2 and 5 % pomace also demonstrated significantly improved emulsifying activity compared to the control. However, at 10 % pomace, the EAI slightly declined to a level higher than the control. A similar trend was observed for ESI, which peaked at 2 % ((25.5±0.1) min) and remained significantly enhanced at 10 % (Fig.1b). According to our results, moderate pomace addition (~2 %) most effectively stabilises emulsions by forming a cohesive interfacial film with optimal viscosity. It seems that further increases in particle content disrupt the film or hinder protein redistribution.

Antioxidant properties

The enrichment of SPCs with black mulberry pomace significantly ($p<0.001$) enhanced their in vitro antioxidant properties, as evidenced by increased total flavonoid content (TFC), total phenolic content (TPC), ABTS and DPPH radical scavenging activities, and ferrous ion (Fe^{2+}) chelation

capacity (Fig. 2). The highest TFC was observed at the 2 % inclusion level (752.31 μg QE/g; Fig. 2a), whereas TPC reached a maximum at 5 % pomace (27.80 mg GAE/g; Fig. 2b). Both ABTS and DPPH activities increased from 1 to 5 % enrichment, followed by a slight decline at 10 % (Fig. 2c and Fig. 2d). In contrast, Fe^{2}-chelating activity peaked at 1 % and decreased at higher pomace levels (Fig. 2e).

Fig. 2

These results emphasize the contribution of phenolic compounds from black mulberry pomace to the antioxidant potential of SPCs. However, the non-linear trends, particularly the decline at 10 % enrichment, are consistent with two phenomena reported in protein-polyphenol systems: (*i*) a masking effect, in which the binding of phenolics to proteins reduces the measurable antioxidant capacity due to the reduced accessibility of phenolic -OH groups to radicals [*36-38*], and (*ii*) the formation of aggregated or insoluble complexes at high phenolic loads, which limits their dispersion and reactivity in solution assays [*38*]. For example, binding of epigallocatechin gallate or gallic acid to β-casein reduced ABTS radical-scavenging activity by ~20 %, and by ~21 % when bound to albumin [*36*]. Also, β-casein-chlorogenic acid complexes exhibited lower ABTS radical-scavenging activity than the sum of their free forms, while FRAP values even showed a synergistic effect, indicating assay-dependent differences in antioxidant outcomes [*36*]. These findings suggest that moderate pomace enrichment (1–5 %) optimizes antioxidant activity, while higher concentrations may diminish it due to structural constraints and phenolic overloading.

In vitro digestibility

While antioxidant properties reflect the bioactive potential of SPCs enriched with black mulberry pomace, their nutritional quality also depends on protein accessibility during digestion. Therefore, *in vitro* digestibility was assessed to evaluate the impact of phenolic compounds, dietary fibres, and their interactions with proteins on enzymatic hydrolysis efficiency. As presented in Fig. 3, the *in vitro* protein digestibility of soy protein concentrates was significantly ($p<0.05$) influenced by the incorporation of black mulberry pomace.

Fig. 3

The control sample (0 %) exhibited the highest digestibility. With increasing pomace content, digestibility progressively declined, reaching a minimum at 5 %, followed by a slight increase at 10 %. However, all values remained significantly ($p<0.05$) lower than the control. The observed reduction in

in vitro digestibility with increasing pomace levels is consistent with previous reports [*39,40*], which indicate that polyphenols can form stable complexes with proteins, thereby reducing their susceptibility to proteolytic enzymes. Such interactions occur through hydrogen bonding, hydrophobic forces, and, in some cases, covalent linkages. This may lead to protein aggregation or the formation of insoluble matrices that limit enzyme accessibility to peptide bonds. In addition, the increase in water-holding capacity, especially at 1 % enrichment (Fig. 1c), may indicate enhanced hydration yet also suggest a denser protein-fibre network that impedes enzyme diffusion. Furthermore, the accumulation of insoluble carbohydrates with increasing pomace levels may further contribute to the physical encapsulation of proteins, thereby reducing their availability for proteolytic digestion.

Despite the observed reduction in digestibility, the inclusion of mulberry pomace enhances the nutritional profile of SPCs by contributing dietary fibre, phenolic compounds, and antioxidant capacity. Therefore, in designing functional food products, a balance should be sought between protein digestibility and the incorporation of health-promoting bioactive components.

Colour analysis

In addition to affecting nutritional accessibility, the incorporation of black mulberry pomace also altered the visual characteristics of SPCs. Colour analysis was conducted to quantify these changes and to explore the influence of phenolic pigments, particularly anthocyanins, and their interactions with the protein-fibre matrix on the chromatic attributes of the samples. The progressive incorporation of black mulberry pomace into soy protein concentrates resulted in significant ($p<0.05$) changes in colour attributes (Table 2). Lightness (L^*) values decreased markedly from 90.29 in the control sample to 71.72 in the 10 % formulation, indicating sample darkening. The a^* values (red–green axis) shifted from -0.65 (slightly green) to 1.90, reflecting increased redness with higher pomace levels. In contrast, the b^* values (yellow–blue axis) remained relatively stable across all treatments.

Table 2

To further elucidate the origin of these colour changes, monomeric anthocyanins were quantified using the pH differential method. They were detected only in the 5 and 10 % pomace-enriched SPCs (0.008 and 0.50 mg/100g, respectively; data not shown). This indicates that most anthocyanins were present in bound or polymerized forms. Such forms are typically stabilised through non-covalent interactions with proteins and polysaccharides (via hydrogen bonding, hydrophobic and electrostatic forces) and are not pH-responsive [*19,41,42*]. Despite their lack of detection by this assay, bound and polymerized anthocyanins can still contribute to visible redness (as evidenced by

the increase in *a**), darkening (decrease in *L**), and overall colour change (increase in *ΔE*) through pigment-matrix associations and co-pigmentation with other phenolics. For mulberry anthocyanins, phenolic-acid co-pigmentation has been shown to intensify colour and improve stability. Namely, Chen *et al*. [*43*] demonstrated that intermolecular co-pigmentation of mulberry anthocyanins with phenolic acids (*e.g.* ferulic and caffeic acids) significantly enhanced colour intensity (*e.g*. ~53 % hyperchromic effect) and stability via mechanisms such as hydrogen bonding and π–π stacking. At the highest pomace level, the saturation of binding sites may have allowed a small fraction of anthocyanins to remain free, thereby becoming detectable by the pH differential method.

FTIR analysis

FTIR spectroscopy (Fig. 4) was used to investigate structural modifications in SPCs induced by the incorporation of black mulberry pomace. Across all samples, the FTIR spectra (Fig 4a and Fig. 4b) displayed well-defined absorption features typical of protein-rich plant matrices, with a broad O-H stretching band near 3300 cm^{-1}, C-H stretching vibrations around 2925 cm^{-1}, and prominent amide bands at ~1650 cm^{-1} (amide I), ~1540 cm^{-1} (amide II), and ~1240 cm^{-1} (amide III) [*27,44*]. These signals collectively reflect contributions from the polypeptide backbone of soy proteins, hydroxyl-bearing phenolic constituents, and carbohydrate-derived structures such as pectins and hemicelluloses.

Fig. 4

Significant shifts were observed (Fig. 4 and Table S1). The O-H band exhibited a pronounced red shift (-104 cm^{-1} at 10 % pomace), indicative of enhanced hydrogen bonding with pomace-derived hydroxyl groups. The amide I band remained unshifted ($\Delta\nu$=0 cm^{-1}), suggesting preservation of the global α-helix/β-sheet composition. The amide II band shifted upward by approx. +12 cm^{-1}, suggesting alterations in N-H bending and C-N stretching consistent with modification of the protein hydrogen bonding network due to protein-polyphenol and protein-fibre interactions (*43*). The I_{1650}/I_{1540} ratio remained nearly constant (1.15 *vs.* 1.17; Table S1), implying no substantial change in secondary structure. However, minor rearrangements cannot be ruled out. Changes in amide III and C-O bands suggest integration of pomace polysaccharides (*e.g.* pectins, hemicellulose) into the SPC matrix. These findings align with well-established FTIR interpretive principles: amide I (mainly C=O stretching) and amide II (N-H bending and C-N stretching) are sensitive to secondary structure and hydrogen bonding. However, amide II is less quantitative than amide I [*44*].

FTIR results indicate that the addition of mulberry pomace strengthens hydrogen-bonded networks and causes minor conformational shifts in SPCs. At 1 % pomace, the red shift of O-H and the upshift of amide II bands coincided with the highest WHC, suggesting that stronger hydrogen bonding increased the number of hydrophilic binding sites. Changes in the amide II and C-O stretching region (~1050–1150 cm^{-1}) also indicate the exposure of hydrophobic domains and the incorporation of carbohydrate structures, both relevant for interfacial activity. At low pomace levels (1–2 %), these adjustments appear to promote protein adsorption and film formation at the oil–water interface, thereby supporting a higher emulsifying capacity and stability. At higher levels (5–10 %), stronger hydrogen bonding and matrix rigidity may restrict protein flexibility and diffusion. This can explain the decline in EAI relative to 1 %, while remaining above the control, despite stable ESI.

Microstructure (SEM) and relation to FTIR and functional properties

Scanning electron micrographs (SEM) revealed progressive microstructural changes in SPCs upon pomace incorporation (Fig. 5). The control (Fig. 5a) displayed relatively compact protein domains with smooth surfaces. At 1 % addition, the matrix appeared more open and discretized with fine pores and discontinuities enhancing water access (Fig. 5b). This morphology aligns with the highest WHC observed at 1 % (Fig. 1). Consistently, FTIR spectra (Fig. 4) showed protein backbone bands together with broad O-H/N-H stretching and C-H stretching regions, reflecting contributions of phenolics and carbohydrate moieties.

Fig. 5

At the addition of 5 % pomace, SEM images (Fig. 5c) showed thicker lamellae and incipient agglomeration of particulates embedded within the protein matrix. This coincided with partial recovery of WHC and OHC (Fig. 1), suggesting capillary retention within fibre-rich domains and exposure of hydrophobic patches capable of binding oil. FTIR confirmed the incorporation of carbohydrate- and phenolic-associated structures. The heterogeneity observed at this inclusion level, with porous corridors juxtaposed against denser clusters, may favour water and oil retention while maintaining interfacial stability.

At 10 %, SEM (Fig 5.d) indicated pronounced aggregation and dense, compacted regions interspersed with larger voids. This morphology corresponds with reduced EAI and plateauing of antioxidant activity (Fig. 2). Increased viscosity and reduced protein mobility likely limited interfacial adsorption. FTIR spectra remained dominated by amide bands, but enhanced O-H and carbohydrate-associated bands suggested tighter polyphenol-polysaccharide-protein associations. These

complexes, together with denser domains, likely hindered enzyme penetration, explaining the reduced digestibility (Fig. 3).

Microstructural and chemical associations can also explain colour changes. Increasing pomace reduced *L** while increasing *a** and chroma values. Anthocyanin-rich particles, visible in SEM as darker inclusions (5–10 %), contributed to both light absorption/scattering as well as the broad O-H band. Their co-localisation within compacted regions may stabilise colour but simultaneously reduce enzyme accessibility.

Correlation and multivariate analysis

To integrate the results obtained from this investigation and gain a comprehensive understanding of the interrelationship between individual parameters, correlation analysis (Fig. S1), principal component analysis (PCA; Fig. 6a and Fig. 6b), and hierarchical cluster analysis (HCA; Fig. 6c) were applied.

Fig. 6

Pearson's correlation analysis showed clear relationships between the chemical composition, techno-functional properties, antioxidant activity, and colour parameters of soy protein concentrates enriched with black mulberry pomace. DPPH and ABTS radical-scavenging activities were perfectly correlated (r=1.00). Both parameters showed strong positive correlations with TPC (r=0.88), whereas correlations with TFC were moderate (r=0.59-0.61). Water-soluble and acid-hydrolysable sugars expressed very strong positive correlations with DPPH and ABTS (r=0.97-1.00). This suggested that sugar-rich matrices co-varied with enhanced antioxidant responses. In contrast, *in vitro* protein digestibility showed very strong negative correlations with DPPH and ABTS (r=-0.96 for both), TPC (r=-0.97), and WS/HS sugars (r=-0.94 and -0.91, respectively). This indicated that polyphenol-protein and fibre-protein interactions may limit enzymatic accessibility. Among functional properties, total protein content correlated very strongly with ESI (r=0.92) and strongly with EAI (r=0.81). In contrast, its relationship with WHC was weak (r=0.29).

According to the results of this study, the soluble protein emerged as a key parameter that showed very strong positive correlations with Fe^{2+}-chelating capacity (r=0.99) and strong correlations with WHC and OHC (both r=0.84). Also, strong correlations with DPPH and ABTS activities (r=0.76 for both) were detected. In addition, SP was very strongly and negatively correlated with digestibility (r=-0.87), highlighting its role in both antioxidant potential and protein accessibility.

Colour parameters were closely linked to the SPCs' composition. Fibre and oil contents were very strongly correlated with redness (*a**; r=0.98/0.97) and very strongly and negatively correlated with lightness (*L**; r=-0.89/-0.98). Digestibility showed a moderate positive association with *L** (r=0.65) and a weaker negative correlation with *a** (r=-0.49). These co-variations consistently indicate that mulberry pomace enrichment reshapes the protein-polyphenol-fibre network, simultaneously influencing antioxidant responses, colour, and digestibility.

Principal component analysis (PCA; Fig. 6a and Fig. 6b) was applied to reduce the dimensionality of the dataset and to elucidate the relationships among physicochemical, functional, antioxidant, and colour parameters of soy protein concentrates enriched with black mulberry pomace. The first two principal components explained 83.6 % of the total variance, with PC1 accounting for 56.7 % and PC2 for 26.9 %, indicating that these components adequately describe the variability within the dataset.

PC1 primarily represented a compositional and biofunctional gradient that clearly separated samples according to pomace addition level. Samples enriched with higher proportions of pomace were positioned on the negative side of PC1 and were associated with increased total phenolic content, antioxidant activity (ABTS, DPPH and TAC), oil and fibre content, as well as higher oil-holding capacity. In contrast, the control sample was located on the positive side of PC1, where it was associated with higher *in vitro* digestibility, moisture content, and higher *L** values, indicating a lighter colour.

PC2 further contributed to the differentiation of samples and was influenced by a combination of protein-related, functional, and colour parameters. The positive side of PC2 was associated with higher protein-related functionality and emulsifying properties, while negative PC2 values were linked to compositional characteristics such as fibre and lipid fractions, as well as colour intensity. Together, these results indicate that sample distribution in the PCA space was governed by a combination of compositional, functional, and colour-related factors, with a clear distinction between protein functionality and fibre-rich fractions.

Hierarchical cluster analysis (HCA; Fig. 6c) supported the PCA results and confirmed the grouping pattern of the samples. The 1 and 2 % samples formed one subcluster, indicating a high degree of similarity in their overall compositional and functional profiles, while the 5 and 10 % samples formed a second, even more closely related subcluster. These two pomace-containing subclusters

were further grouped together, whereas the control sample remained clearly separated, confirming its distinct physicochemical and functional profile.

PCA and HCA provide an integrated statistical perspective, corroborating trends observed in individual parameters, FTIR and SEM analyses, and correlation patterns. The clustering of samples along biofunctional and compositional axes reinforces the conclusion that even low pomace levels can substantially alter the nutritional and functional properties of SPCs.

CONCLUSIONS

This study demonstrated that the incorporation of black mulberry pomace into soy protein concentrates induced pronounced compositional, structural, and functional modifications. Moderate enrichment, particularly at lower levels, enhanced hydration and emulsifying properties, while simultaneously improving antioxidant capacity. These findings highlight the potential of mulberry pomace as a sustainable ingredient for tailoring the techno-functional profile and bioactivity of soy protein concentrates. The novelty of this work lies in linking microstructural and spectroscopic evidence with functional performance, thereby offering new perspectives for the valorisation of fruit by-products in plant-based protein formulations. Future studies should focus on optimizing pomace incorporation levels in relation to protein digestibility and evaluating the performance of these concentrates in real food systems, in order to further support their application as sustainable functional ingredients.

ACKNOWLEDGEMENTS

The authors gratefully acknowledge the company *Bankom d.o.o.* (Belgrade, Serbia) for generously providing moderately toasted soybean flour used in this study.

FUNDING

The research was carried out within the framework of the "Agreement on the implementation and financing of scientific research in 2025 between the Ministry of Science, Technological Development and Innovation of the Republic of Serbia and the Faculty of Agriculture of the University of Belgrade", number 451-03-137/2025-03/200116.

CONFLICT OF INTEREST

There is no conflict of interest.

SUPPLEMENTARY MATERIALS

All supplementary materials are available at: www.ftb.com.hr.

AUTHORS' CONTRIBUTION

N. Barać was involved in the conception and design of the work, performed the analysis, interpreted the data, and wrote the original draft. B. Rabrenović participated in the conception and design of the work. I. Sredović Ignjatović, S. Lević, V. Pavlović, S. Žilić and D. Milovanović were involved in the analysis and interpretation of data. Miroljub Barać did the critical revision and supervised the work. All authors read and agree upon the final version of the manuscript.

ORCID ID

N. Barać https://orcid.org/0009-0002-7221-9661
B. Rabrenović https://orcid.org/0000-0002-4006-1612
I. Sredović Ignjatović https://orcid.org/0000-0002-2471-9242
S. Lević https://orcid.org/0000-0001-8337-3475
V. Pavlović https://orcid.org/0000-0002-1138-0331
S. Žilić https://orcid.org/0000-0001-8299-9185
D. Milovanović https://orcid.org/0000-0002-6915-2606
M. Barać https://orcid.org/0000-0002-6645-4537

REFERENCES

1. Santos MD, Rocha DAVFD, Bernardinelli OD, Oliveira Júnior FD, de Sousa DG, Sabadini E, *et al.* Understanding the performance of plant protein concentrates as partial meat substitutes in hybrid meat emulsions. Foods. 2022;11(21):3311. https://doi.org/10.3390/foods11213311

2. Tama A, Karaś M. The health-promoting potential of fruit pomace and its application in the confectionery industry. Appl Sci. 2025;15(10):5790. https://doi.org/10.3390/app15105790

3. Lucarini M, Durazzo A, Bernini R, Campo M, Vita C, Souto EB, *et al.* Fruit wastes as a valuable source of value-added compounds: a collaborative perspective. Molecules. 2021;26(21):6338. https://doi.org/10.3390/molecules26216338

4. Pascoalino LA, Barros L, Barreira JC, Oliveira MBP, Reis FS. Closing the loop: Exploring apple pomace as a source of bioactive compounds in the framework of circular economy. Sustain Food Technol. 2025;3:81–95.
https://doi.org/10.1039/d4fb00172a

5. Du H, Yang H, Wang X, Zhu F, Tang D, Cheng J, Liu X. Effects of mulberry pomace on physicochemical and textural properties of stirred-type flavored yogurt. J Dairy Sci. 2021;104(12):12403-14.
https://doi.org/10.3168/jds.2020-20037

6. Raczkowska E, Serek P. Health-promoting properties and the use of fruit pomace in the food industry- a review. Nutrients. 2024;16(16):2757.
https://doi.org/10.3390/nu16162757

7. Santos LFD, Lopes ST, Nazari MT, Biduski B, Pinto VZ, Santos JS, *et al*. Fruit pomace as a promising source to obtain biocompounds with antibacterial activity. Crit Rev Food Sci Nutr. 2023;63(33):12597-609.
https://doi.org/10.1080/10408398.2022.2103510

8. Khodaiyan F, Parastouei K. Co-optimization of pectin and polyphenols extraction from black mulberry pomace using an eco-friendly technique: Simultaneous recovery and characterization of products. Int J Biol Macromol. 2020;164:1025-36.
https://doi.org/10.1016/j.ijbiomac.2020.07.107

9. Shahidi F, Dissanayaka CSW. Phenolic-protein interactions: insight from in-silico analyses – a review. Food Prod Process Nutr. 2023;5 (1):2.
https://doi.org/10.1186/s43014-022-00121-0

10. Xue H, Feng J, Tang Y, Wang X, Tang J, Cai, X, Zhong, H. Research progress on the interaction of the polyphenol–protein–polysaccharide ternary systems. Chem Biol Technol Agric. 2024;11:95.
https://doi.org/10.1186/s40538-024-00632-7

11. AOAC Official Method 984.13. Protein (Crude) in Animal Feed and Pet Food - Kjeldahl Method. Gaithersburg, MD, USA: AOAC International; 2005.

12. AOAC Official Method 930.15. Loss on Drying (Moisture) for Feeds. Gaithersburg, MD, USA: AOAC International; 2019.

13. AOAC Official Method 920.39. Fat (Crude) in Animal Feed - Soxhlet Extraction Method. 18th ed. Gaithersburg, MD, USA: AOAC International; 2005.

14. AOAC Official Method 962.09. Crude fiber in animal feed and pet food. Gaithersburg, MD, USA: AOAC International; 2019.

15. Dubois M, Gilles KA, Hamilton JK, Rebers PA, Smith F. Colorimetric method for determination of sugars and related substances. Anal Chem. 1956;28:350-6.
https://doi.org/10.1021/ac60111a017
16. Bradford MM. A rapid and sensitive method for the quantitation of microgram quantities of protein utilizing the principle of protein-dye binding. Anal Biochem. 1976;72:248-54.
https://doi.org/10.1016/0003-2697(76)90527-3
17. Kostić DA, Dimitrijević DS, Mitić SS, Mitić MN, Stojanović GS, Živanović A. Phenolic content and antioxidant activities of fruit extracts of *Morus nigra* L. (*Moraceae*) from Southeast Serbia. Trop J Pharm Res. 2013;12:105-10.
https://doi.org/10.4314/tjpr.v12i1.17
18. Žilić S, Simić M, Belović M, Škrobot D, Srdić J, Perić V. Chemical, rheological and sensory characteristics of sweet spreads made from by-products of soya bean and maize. Int J Food Sci Technol. 2020;55(4):1559-71.
https://doi.org/10.1111/ijfs.14382
19. Giusti MM, Wrolstad RE. Characterization and measurement of anthocyanins by UV-Visible spectroscopy. Curr Protoc Food Anal Chem. 2001; 00:F1.2.1-F1.2.13.
https://doi.org/10.1002/0471142913.faf0102s00
20. Meira SMM, Daroit DJ, Helfer VE, Corrêa APF, Segalin J, Carro S, Brandelli A. Bioactive peptides in water-soluble extracts of ovine cheeses from Southern Brazil and Uruguay. Food Res Int. 2012;48(1):322-9.
https://doi.org/10.1016/j.foodres.2012.05.009
21. Arnao MB, Cano A, Acosta M. The hydrophilic and lipophilic contribution to total antioxidant activity. Food Chem. 2001;73:239-44.
https://doi.org/10.1016/S0308-8146(00)00324-1
22. SpectraMagic NX software ver. 3.40. Konica Minolta, Inc. Osaka, Japan; 2024. Available from: https://www.konicaminolta.com/instruments/download/software/color/smnx/difference.
23. Barać M, Cabrilo S, Pešić M, Stanojević S, Pavlićević M, Maćej O, Ristić N. Functional properties of pea (*Pisum sativum*, L.) protein isolates modified with chymosin. Int J Mol Sci. 2011;12(12):8372-87.
https://doi.org/10.3390/ijms12128372
24. Gouw VP, Jung J, Zhao Y. Functional properties, bioactive compounds, and *in vitro* gastrointestinal digestion study of dried fruit pomace powders as functional food ingredients. LWT. 2017;80:136-44.
https://doi.org/10.1016/j.lwt.2017.02.015

25. Papillo VA, Vitaglione P, Graziani G, Gokmen V, Fogliano V. Release of antioxidant capacity from five plant foods during a multistep enzymatic digestion protocol. J Agric Food Chem. 2014;62(18):4119-26.
https://doi.org/10.1021/jf500695a
26. Hamzalıoğlu A, Gökmen V. Potential reactions of thermal process contaminants during digestion. Trends Food Sci Technol. 2020;106:198-208.
https://doi.org/10.1016/j.tifs.2020.10.014
27. De Meutter J, De Vleeschouwer K, Van Der Meeren P, *et al*. Insights into protein secondary structure by FTIR spectroscopy. Eur Biophys J. 2021;50:1287-1305.
https://doi.org/10.1007/s00249-021-01507-7
28. IBM SPSS Statistics for Windows, version 26.0. IBM Corp., Armonk, NY, USA; 2019. Available from: https://www.ibm.com/products/spss-statistics.
29. Python language reference, version 3.10. Python Software Foundation, Wilmington, DE, USA; 2021. Available from: https://www.python.org.
30. Barać M, Pešić M, Žilić S, Stanojević S. Soy protein products (in Serbian). Belgrade: University of Belgrade, Faculty of Agriculture, 2014.
31. Saura-Calixto F. Dietary fiber as a carrier of dietary antioxidants: an essential physiological function. J Agric Food Chem. 2011;59(1):43-9.
https://doi.org/10.1021/jf1036596
32. McRorie JW Jr, McKeown NM. Understanding the physics of functional fibers in the gastrointestinal tract: an evidence-based approach to resolving enduring misconceptions about Insoluble and soluble fiber. J Acad Nutr Diet. 2017;117(2):251-64.
https://doi.org/10.1016/j.jand.2016.09.021
33. Gecgel U, Gumus T, Tasan M, Daglioglu O, Arici M. Investigating some physicochemical properties and fatty acid composition of native black mulberry (*Morus nigra* L.) seed oil. J Am Oil Chem Soc. 2011;88:1179-87.
https://doi.org/10.1007/s11746-011-1771-6.
34. Bozdoğan Konuşkan D. Minor bioactive lipids in cold pressed oils. In: Ramadan MF, editor. Cold Pressed Oils. London, UK: Academic Press; 2020. pp. 7-14.
https://doi.org/10.1016/B978-0-12-818188-1.00002-5
35. Elleuch M, Bedigian D, Roiseux O, Besbes S, Blecker C, Attia H. Dietary fibre and fibre-rich by-products of food processing: Characterisation, technological functionality and commercial applications: A review. Food Chem. 2011;124(2):411-21.
https://doi.org/10.1016/j.foodchem.2010.06.077

36. Arts MJTJ, Haenen GRMM, Wilms LC, Beetstra SAJN, Heijnen CGM, Voss HP, Bast A. Interactions between flavonoids and proteins: Effect on the total antioxidant capacity. J Agric Food Chem. 2002;50(5):1184-7.
https://doi.org/10.1021/jf010855a

37. Feng Y, Jin C, Lv S, Zhang H, Ren F, Wang J. Molecular mechanisms and applications of polyphenol–protein complexes with antioxidant properties: A review. Antioxidants. 2023;12(8):1577.
https://doi.org/10.3390/antiox12081577

38. Zhou W, Peng C, Wang D, Li J, Tu Z, Zhang L. Interaction mechanism between OVA and flavonoids with different hydroxyl groups on B-ring and effect on antioxidant activity. Foods. 2022;11(9):1302.
https://doi.org/10.3390/foods11091302

39. Yu J, Mi Y, Ji S. In vitro evaluating the influence of grape seed polyphenol extract on the digestibility of macronutrients. J Health Sci. 2016;4:167-76.
https://doi.org/10.17265/2328-7136/2016.04.001

40. Veličković DT, Rakić VP, Jovanović ST, Miljković MN. Polyphenol-protein interactions: mechanisms, effects on protein functionality and nutritional quality. Food Res Int. 2020;137:109682.
https://doi.org/10.1016/j.foodres.2020.109682

41. Ta TMN, Hoang CH, Nguyen TM, Tran TTT, Ton NMN, Le VVM. Effects of mulberry pomace addition and transglutaminase treatment on the quality of pasta enriched with antioxidants and dietary fiber. Pol J Food Nutr Sci. 2023;73(4):301-10.
https://doi.org/10.31883/pjfns/172244

42. Li J, Wang B, He Y, Wen L, Nan H, Zheng F, *et al*. A review of the interaction between anthocyanins and proteins. Food Sci Technol Int. 2021;27(5):470-82.
https://doi.org/10.1177/1082013220962613

43. Chen X, Gao Q, Liao S, Zou Y, Yan J, Li Q. Co-pigmentation mechanism and thermal reaction kinetics of mulberry anthocyanins with different phenolic acids. Foods. 2022;11(23):3806.
https://doi.org/10.3390/foods11233806

44. Majaliwa G, Kibazohi, O, Alminger, M. FTIR characterization of protein–polyphenol–pectin interactions in banana pulp. Int J Biochem Res Rev. 2025;34(2):1–12.
https://doi.org/10.9734/ijbcrr/2025/v34i2963

Table 1. Chemical composition of soy protein concentrates (SPCs) with varying levels of black mulberry pomace

w(pomace)/%	*w*(TP)/(g/100 g DM)	*w*(SP)/(g/100 g DM)	w(WSS)/(g/100 g DM)	*w*(AHS)/(g/100 g DM)	*w*(fibre)/(g/100 g DM)	*w*(oil)/(g/100 g)	*w*(moisture)/%
0	(71.92±0.34)^{c}	(5.71±0.02)^{c}	(0.33±0.01)^{d}	(6.4±0.0)^{e}	(4.82±0.10)^{e}	(0.75±0.02)^{c}	(11.2±0.2)^{a}
1	(74.45±0.52)^{b}	(9.89±0.15)^{a}	(0.43±0.06)^{c}	(12.71±0.14)^{d}	(5.37±0.18)^{d}	(0.82±0.04)^{b}	(10.3±0.2)^{b}
2	(76.07±0.35)^{a}	(9.61±0.26)^{a}	(0.6±0.0)^{b}	(14.43±0.03)^{c}	(6.12±0.22)^{c}	(0.87±0.07)^{b}	(11.1±0.1)^{a}
5	(72.64±0.62)^{c}	(9.53±0.08)^{a}	(0.65±0.01)^{a}	(17.15±0.15)^{b}	(8.05±0.31)^{b}	(1.20±0.10)^{a}	(10.6±0.1)^{b}
10	(72.4±0.1)^{c}	(8.66±0.03)^{b}	(0.7±0.0)^{a}	(18.86±0.86)^{a}	(11.34±0.15)^{a}	(1.30±0.05)^{a}	(10.5±0.3)^{b}

TP=total proteins, SP=soluble proteins, WSS=water-soluble sugar, AHS=acid-hyrolysable sugars, DM=dry matter. Values are mean±S.D. Different superscript letters in the same column indicate statistically significant differences ($p<0.05$)

Table 2. Color parameters of soy protein concentrates enriched with mulberry pomace

w(pomace)/%	*L**	*a**	*b**	*C**	*h*°	Δ*E*
0	(90.29±0.34)^{a}	(-0.65± 0.1)^{e}	(11.26±0.45)^{b}	(11.28±0.44)^{b}	(93.32±1.13)^{a}	(0.000)^{d}
1	(82.72±0.37)^{b}	(0.51± 0.07)^{d}	(12.35±0.36)^{a}	(12.36±0.37)^{a}	(87.63±1.13)^{b}	(7.74±0.34)^{c}
2	(82.17±0.47)^{b}	(0.263±0.09)^{c}	(10.72±0.37)^{b}	(10.72±0.38)^{b}	(88.59±1.11)^{b}	(8.19±0.37)^{c}
5	(76.04±0.37)^{c}	(1.12±0.06)^{b}	(10.57± 0.39)	10.63±0.39)^{b}	(83.97±1.17)^{c}	(14.38±0.42)^{b}
10	(71.72±0.32)^{d}	(1.89± 0.07)^{a}	(12.16±0.42)^{a}	(12.31±0.43)^{a}	(81.13±1.15)^{c}	(18.77±0.48)^{a}

Values are expressed as mean±S.D. Color parameters include lightness (*L**), red-green coordinate (*a**), yellow-blue coordinate (*b**), chroma (*C**), hue angle (*h*°), and total color difference (Δ*E*)

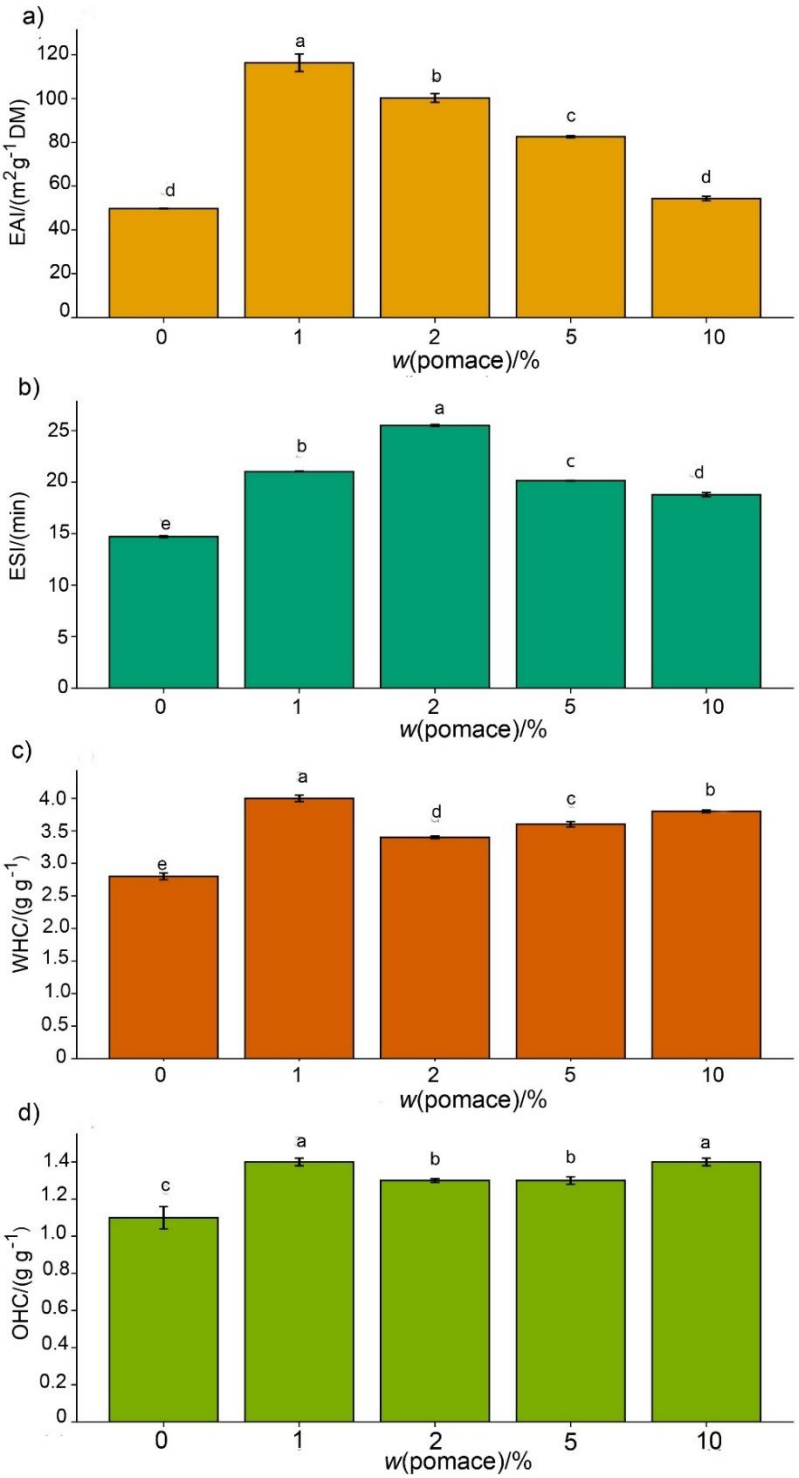

Fig. 1. Techno-functional properties of soy protein concentrates enriched with 0, 1, 2, 5 and 10 % black mulberry pomace: a) emulsifying activity index (EAI), b) emulsion stability index (ESI), c) water-holding capacity (WHC), and d) oil-holding capacity (OHC). Values are expressed as mean±S.D. Different letters indicate significant differences ($p<0.05$). All values are reported on a dry matter basis

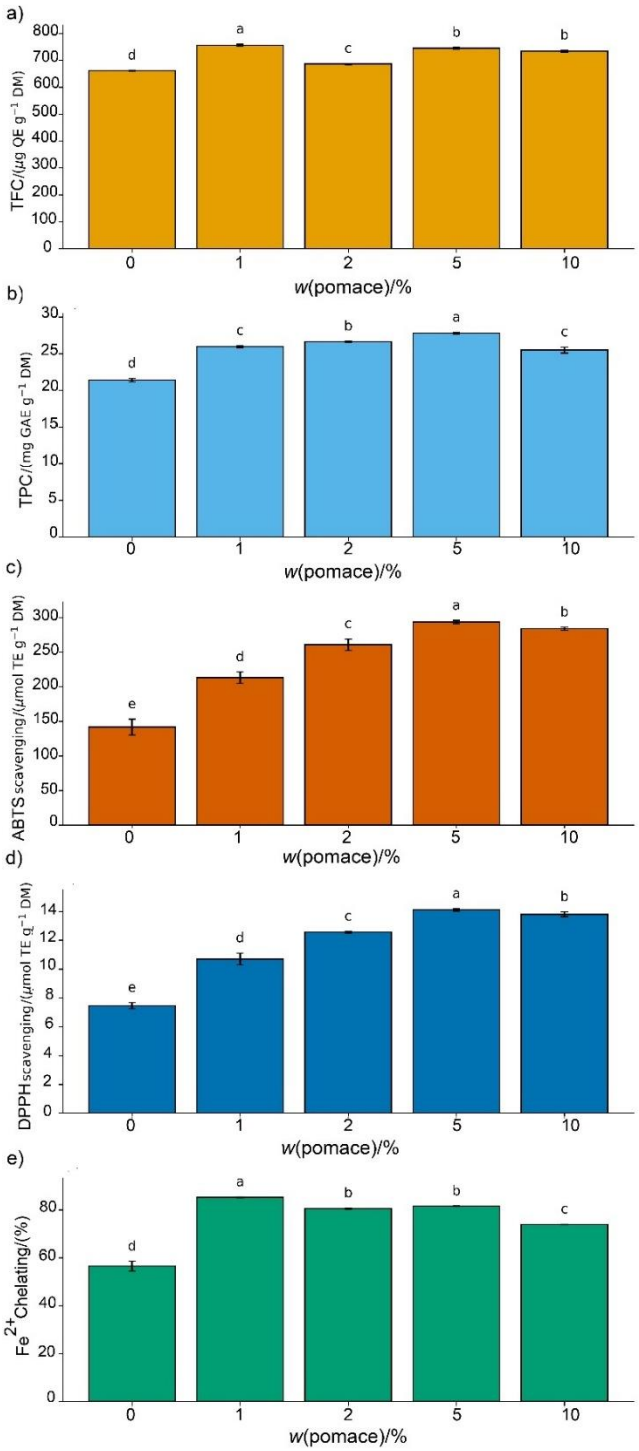

Fig. 2. Antioxidant properties of soy protein concentrates with 0–10 % black mulberry pomace: a) total flavonoid content (TFC), b) total phenolic content (TPC), c) ABTS radical scavenging activity, d) DPPH radical scavenging activity, and e) Fe^{2+}-chelating activity. Values are expressed as mean±S.D. Different letters above bars indicate significant differences ($p<0.05$)

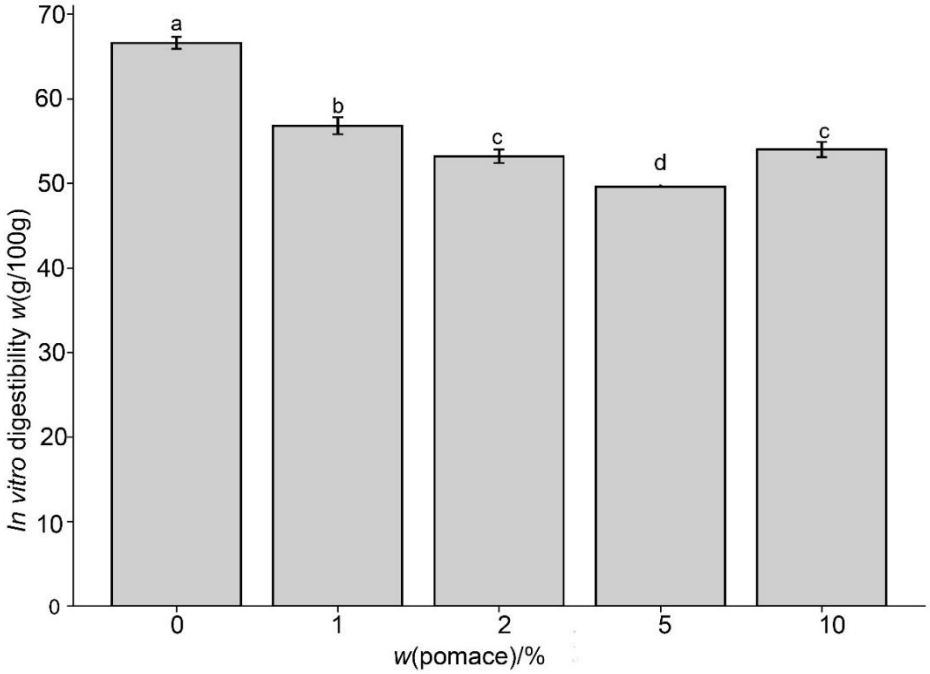

Fig. 3. *In vitro* digestibility of soy protein concentrates enriched with black mulberry pomaces. Values are expressed as mean±S.D. Different letters above bars indicate significant differences ($p<0.05$)

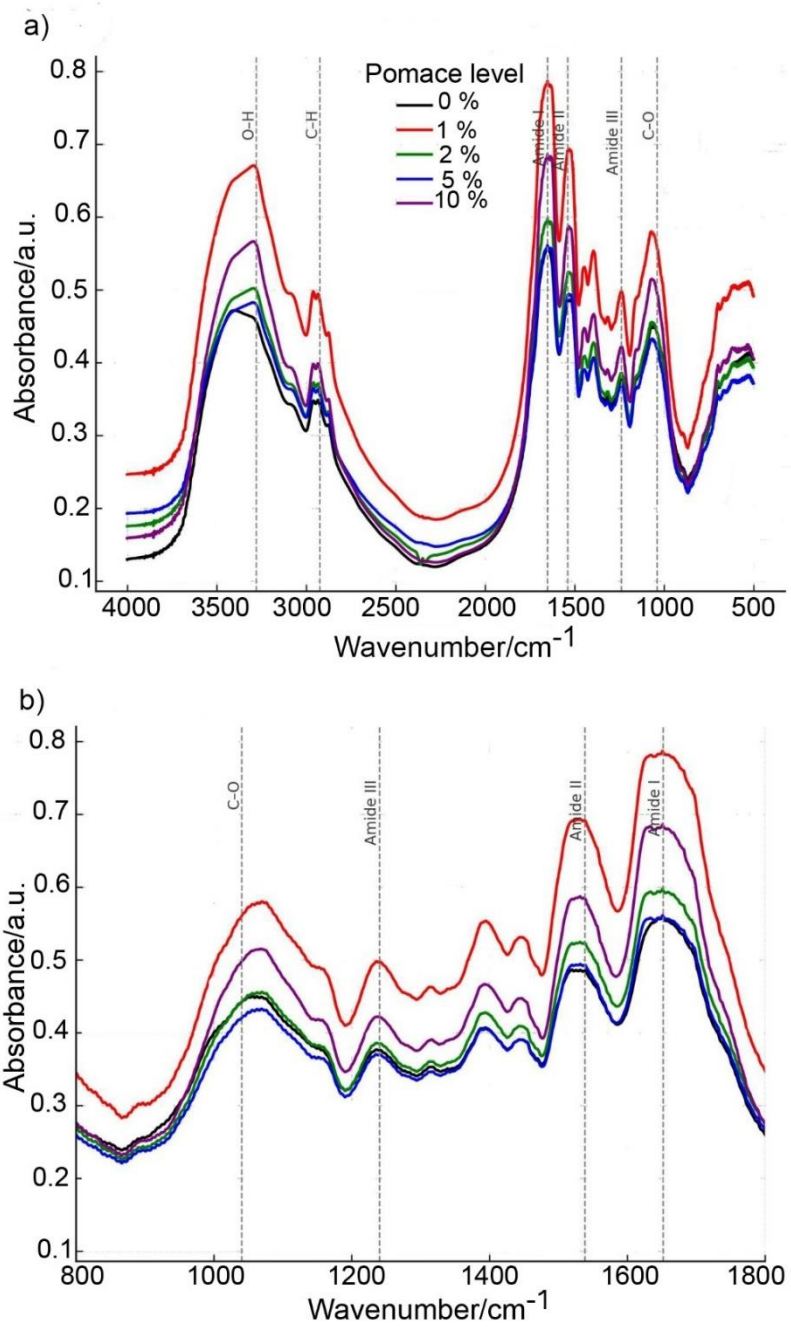

Fig. 4. FTIR spectra of soy protein concentrates with 0–10 % black mulberry pomace: a) full spectra (4000–600 cm^{-1}), b) expanded region highlighting main absorption bands

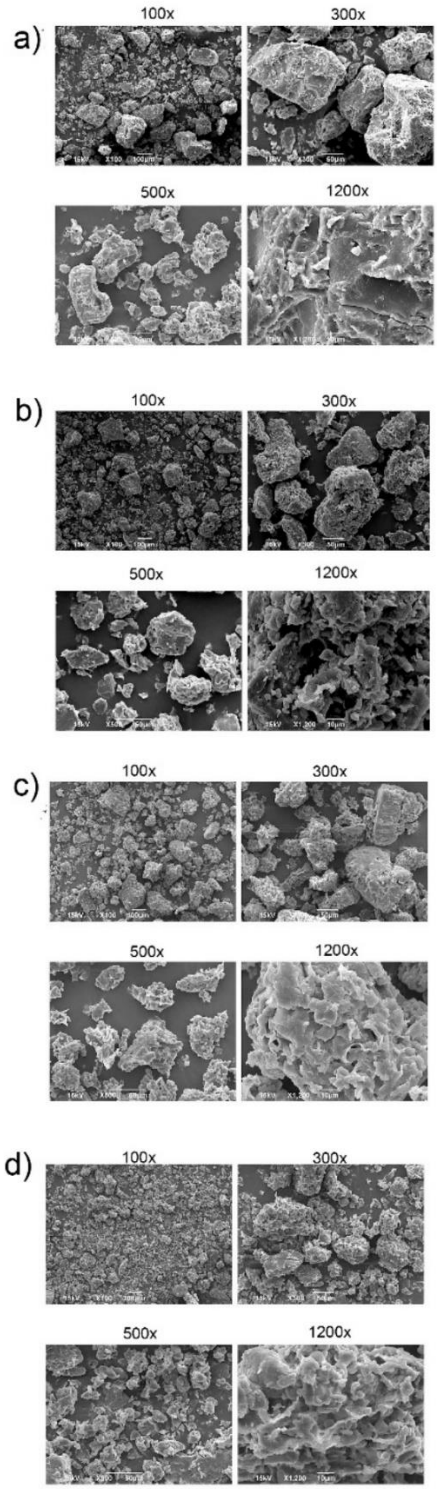

Fig. 5. Scanning electron micrographs (SEM) of soy protein concentrates with 0–10 % black mulberry pomace at different magnifications: a) 0 %, b) 1 %, c) 5 %, and d) 10 % pomace. Each panel shows images at 100×, 300×, 500× and 1200× magnification

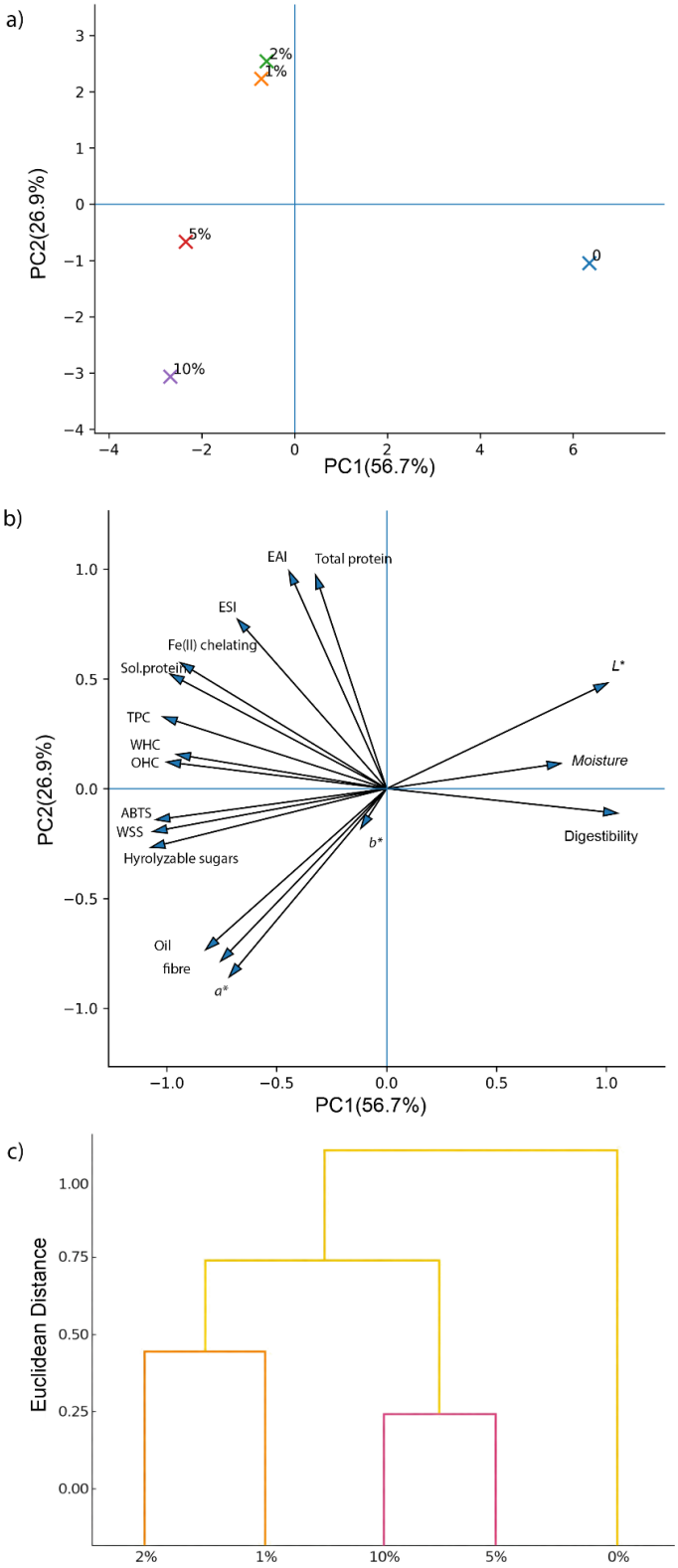

Fig. 6. Multivariate analysis of soy protein concentrates with 0–10 % black mulberry pomace: a) PCA score plot, b) PCA loading plot, and c) hierarchical cluster analysis (HCA) dendrogram

SUPPLEMENTARY MATERIAL

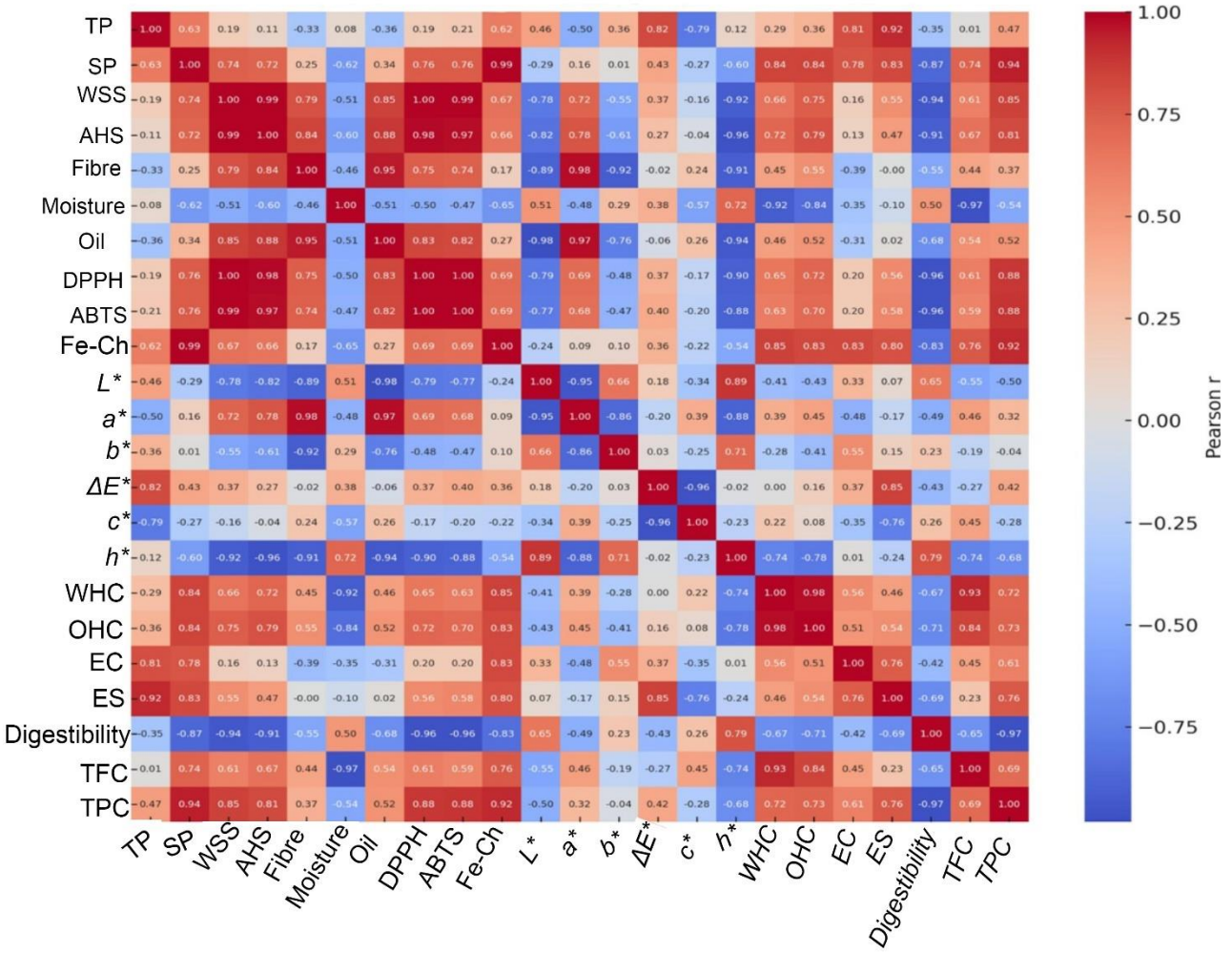

Fig. S1. Correlation heatmap showing Pearson correlation coefficients ($p<0.05$) between chemical composition, techno-functional, antioxidant and digestibility parameters of soy protein concentrates with 0–10 % black mulberry pomace. TP=total protein, SP=soluble protein, WSS=water-soluble sugar, AHS=acid-soluble sugar, ABTS=radical scavenging activity, Fe-Ch=Fe(II)=chelating ability, WHC=water holding capacity, OHC=oil holding capacity, DPPH=radical scavenging activity, TFC=total phenol content, TFC=total flavonoid content, *L**=lightness, *a**=red-green coordinate, *b**=yellow-blue coordinate, *C**=chroma, *h*°=hue angle, Δ*E*=total color difference

Table S1. Characteristic FTIR absorption bands of soy protein concentrates with different levels of mulberry pomace and their shifts relative to the control (0 % pomace)

Functional group (Region/cm^{-1})	0 % ν_{max} /cm^{-1}	0 % $\Delta\nu$ vs 0 % (cm^{-1})	1 % ν_{max}/cm^{-1}	1 % $\Delta\nu$ vs 0 % (cm^{-1})	2 % ν_{max}/cm^{-1}	2 % $\Delta\nu$ vs 0 % (cm^{-1})	5 % ν_{max}/cm^{-1}	5 % $\Delta\nu$ vs 0 % (cm^{-1})	10 % ν_{max}/cm^{-1}	10 % $\Delta\nu$ vs 0 % (cm^{-1})
O–H (3700–3000)	3400.50	0.00	3292.49	-108.01	3294.42	-106.08	3294.42	-106.08	3296.35	-104.16
C–H (2970–2850)	2933.73	0.00	2960.73	27.00	2960.73	27.00	2958.80	25.07	2933.73	0.00
Amide I (1700–1600)	1651.07	0.00	1651.07	0.00	1651.07	0.00	1651.07	0.00	1651.07	0.00
Amide II (1580–1480)	1519.91	0.00	1531.48	11.57	1531.48	11.57	1531.48	11.57	1531.48	11.57
Amide III (1300–1200)	1236.37	0.00	1236.37	0.00	1236.37	0.00	1234.44	-1.93	1236.37	0.00
C–O (1150–1000)	1055.06	0.00	1070.49	15.43	1068.56	13.50	1068.56	13.50	1068.56	13.50
I_{1650}/I_{1540}	1.15		1.13		1.14		1.14		1.17	

Negative values indicate a shift to lower wavenumbers compared to the control (0 % pomace)